Report

Cell Reports

Astrocyte Depletion Impairs Redox Homeostasis and Triggers Neuronal Loss in the Adult CNS

Graphical Abstract

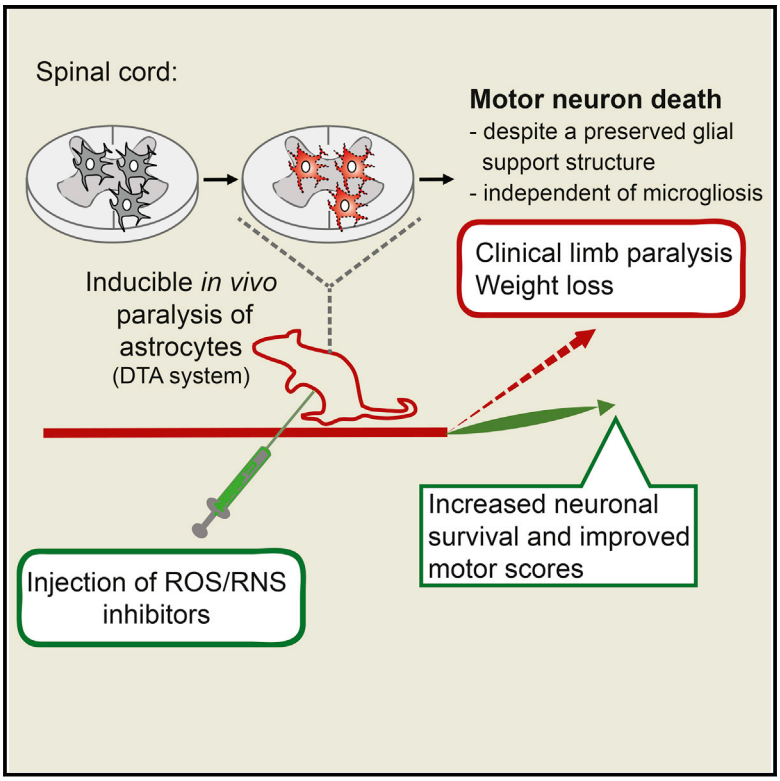

Highlights

- When adult GFAP$^+$ astrocytes are depleted in vivo, motor skills are severely impaired
- Neuronal loss occurs, whereas astroglial structural support still persists
- Astroglial dysfunction disrupts CNS redox homeostasis, independent of microgliosis
- Neutralization of ROS/RNS protects from neuronal injury

Authors

Bettina Schreiner, Elisa Romanelli, Pawel Liberski, ..., Frank Heppner, Martin Kerschensteiner, Burkhard Becher

Correspondence

becher@immunology.uzh.ch

In Brief

Schreiner et al. examine the functional contribution of astrocytes to tissue homeostasis in the adult CNS and identify the redox-scavenging capacity of GFAP$^+$ astrocytes as a key factor for neuronal health in vivo. The importance of the metabolic integrity of the glia-neuron interface highlights potential therapies for the treatment of neurodegenerative diseases.

Schreiner et al., 2015, Cell Reports *12*, 1377–1384
September 1, 2015
http://dx.doi.org/10.1016/j.celrep.2015.07.051

CellPress

Cell Reports
Report

Astrocyte Depletion Impairs Redox Homeostasis and Triggers Neuronal Loss in the Adult CNS

Bettina Schreiner,[1,2] Elisa Romanelli,[3] Pawel Liberski,[4] Barbara Ingold-Heppner,[5] Bettina Sobottka-Brillout,[1,6] Tom Hartwig,[1] Vijay Chandrasekar,[7] Helge Johannssen,[8] Hanns Ulrich Zeilhofer,[8,9] Adriano Aguzzi,[7] Frank Heppner,[10] Martin Kerschensteiner,[3,11] and Burkhard Becher[1,*]

[1]Institute of Experimental Immunology, University of Zurich, 8057 Zurich, Switzerland
[2]Department of Neurology, University Hospital Zurich, 8091 Zurich, Switzerland
[3]Institute of Clinical Neuroimmunology, Ludwig-Maximilians Universität München, 81377 Munich, Germany
[4]Department of Molecular Pathology and Neuropathology, Medical University of Lodz, 92-101 Lodz, Poland
[5]Department of Pathology, Charité-Universitätsmedizin Berlin, 10117 Berlin, Germany
[6]Institute of Surgical Pathology, University Hospital Zurich, 8091 Zurich, Switzerland
[7]Institute of Neuropathology, University Hospital Zurich, 8091 Zurich, Switzerland
[8]Institute of Pharmacology and Toxicology, University of Zurich, 8057 Zurich, Switzerland
[9]Institute of Pharmaceutical Sciences, Swiss Federal Institute of Technology (ETH), 8093 Zurich, Switzerland
[10]Department of Neuropathology, Charité-Universitätsmedizin Berlin, 10117 Berlin, Germany
[11]Munich Cluster for Systems Neurology (SyNergy), 81377 Munich, Germany
*Correspondence: becher@immunology.uzh.ch

http://dx.doi.org/10.1016/j.celrep.2015.07.051

SUMMARY

Although the importance of reactive astrocytes during CNS pathology is well established, the function of astroglia in adult CNS homeostasis is less well understood. With the use of conditional, astrocyte-restricted protein synthesis termination, we found that selective paralysis of GFAP$^+$ astrocytes in vivo led to rapid neuronal cell loss and severe motor deficits. This occurred while structural astroglial support still persisted and in the absence of any major microvascular damage. Whereas loss of astrocyte function did lead to microglial activation, this had no impact on the neuronal loss and clinical decline. Neuronal injury was caused by oxidative stress resulting from the reduced redox scavenging capability of dysfunctional astrocytes and could be prevented by the in vivo treatment with scavengers of reactive oxygen and nitrogen species (ROS/RNS). Our results suggest that the subpopulation of GFAP$^+$ astrocytes maintain neuronal health by controlling redox homeostasis in the adult CNS.

INTRODUCTION

Astrocytes are specialized glial cells of the CNS that vastly outnumber neurons. Different astrocyte subtypes have been described, of which some express the cytoskeletal protein glial fibrillary acidic protein (GFAP). GFAP$^+$ astrocytes extend many long fiber-like processes, which form gap junctions between neighboring astrocytes, contact synapses, and nodes of Ranvier, and surround blood vessels. Astrocytes likely are important contributors to neurodegenerative disease such as familial amyotrophic lateral sclerosis (Haidet-Phillips et al., 2011) or certain types of leukodystrophies. But it has also been proposed that they have essential functions in the healthy CNS, including the maintenance of neuronal homeostasis, the regulation of synaptic transmission, and the formation of the neurovascular unit (reviewed in Allen and Barres, 2009 and Sofroniew and Vinters, 2010). Much of what we know about astrocyte function has come from in vitro studies using isolated glial cells or slice cultures, where they among others promote growth and survival of neurons (Banker, 1980). More-recent studies have shown that astrocytes can also support CNS myelination in multiple culture models (Sorensen et al., 2008). However, gene targeting of astrocyte intermediate filament genes like GFAP and vimentin resulted in no gross neurological, behavioral, or structural CNS abnormalities in vivo (Colucci-Guyon et al., 1994; Pekny et al., 1995). Reactive astrocytes have been specifically depleted during scar formation using the GFAP-HSV-TK model, resulting in exacerbated traumatic brain injury, whereas it also improved nerve fiber outgrowth (Bush et al., 1999). Furthermore, diphtheria toxin (DT)-A-mediated astrocyte depletion has revealed astroglial regulation of synaptogenesis in the developing nervous system (Tsai et al., 2012).

In the present study, we sought to use genetic strategies for selective in vivo paralysis and depletion to interrogate the proposed functional contribution of GFAP$^+$ astrocytes to tissue homeostasis in the adult CNS.

RESULTS

Inducible Paralysis of Adult GFAP$^+$ Astrocytes In Vivo

In order to study the role of astrocytes under physiological conditions in adult mice in vivo, we used two different models of astrocyte targeting: we crossed mice in which expression of the DT receptor (DTR) from an ubiquitously active promoter is prevented by a *loxP*-flanked stop cassette (iDTR; Buch et al.,

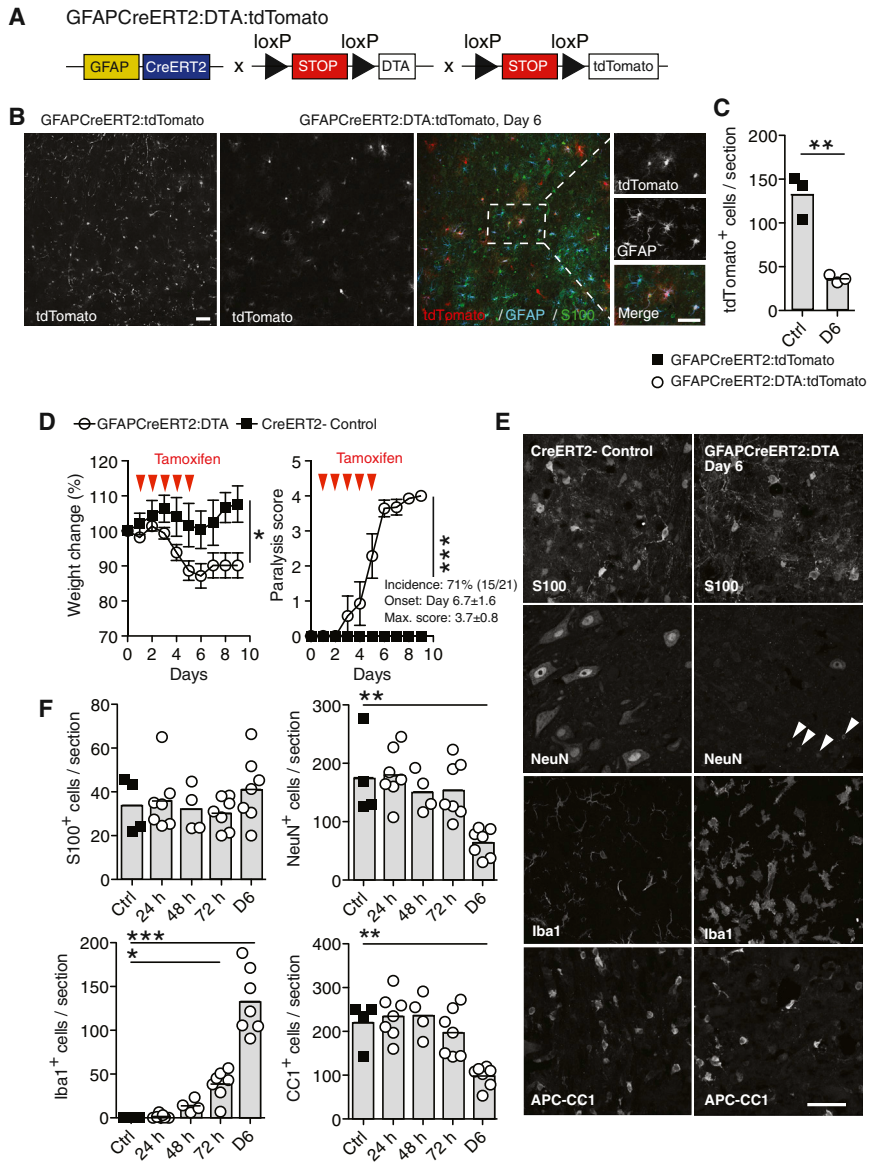

Figure 1. Paralysis of Astrocytes in GFAP-CreERT2:DTA Mice Leads to a Rapid and Severe Neuronal Motor Phenotype

(A) Schematic diagram of GFAPCreERT2 × DTA (GFAPCreERT2:DTA) mice, crossed with Rosa26-tdTomato transgenic reporter mice (Ai14) to label cells in which Cre-mediated recombination takes place. Tamoxifen i.p. injections were performed at days 1–5.

(B and C) Spinal cord samples were immunostained for GFAP and S100, and the numbers of tdTomato$^+$ cells as well as their co-localization with the astrocyte marker proteins were quantified.

(B) Representative images of tdTomato$^+$ cells in sections from control GFAPCreERT2:tdTomato mice and mice in which the DTA expression is additionally activated (GFAPCreERT2:DTA:tdTomato) are shown. The insets show tdTomato$^+$ cells with astrocytic morphology and co-localizing with GFAP. The number of tdTomato$^+$ astrocytes per section were significantly reduced at day 6 in GFAPCreERT2:DTA:tdTomato-D6 compared to GFAPCreERT2:tdTomato-Ctrl mice. For quantifications, see (C). In (C), squares and circles represent individual mice and the bar the mean value (n = 3/group; two-tailed Student's t test).

(D–F) GFAPCreERT2:DTA mice were i.p. injected with tamoxifen at days 1–5. (D) At days 5–8, mice exhibited a severe paralysis that rapidly progressed to all four limbs and was accompanied by weight loss (mean ± SEM; n = 3–7/group; two-way ANOVA test). (E and F) Cervical sections were immunostained at the indicated time points to assess remaining astrocyte structural integrity (S100) and to detect neurons (NeuN), oligodendrocytes (APC-CC1), and microglia (Iba1). Arrows in (E) indicate neurons undergoing cell death. For quantifications, see (F). Values of individual mice are shown by circles (GFAPCreERT2:DTA; n = 4–7 mice/time point) and squares (CreERT2$^-$ control tissue; n = 4). Group means are indicated by bars. Statistical analyses were performed via one-way ANOVA and Dunnett's multiple comparison test versus Ctrl. *p < 0.05; **p < 0.01; ***p < 0.001.

The scale bars represent 200 μm (B), 50 μm (inset in B), and 50 μm (E). See also Figures S1 and S2.

2005) with transgenic mice expressing the Cre recombinase under the control of the GFAP promoter (GFAPCre:iDTR; Figure S1). This led to DTR expression selectively by GFAP$^+$ astrocytes. DT is a toxin that, upon entry into the cytoplasm, "paralyzes" target cells by catalyzing the inactivation of elongation factor 2, resulting in termination of protein synthesis and subsequent cell death (Honjo et al., 1971).

Because glial cells are the progenitors for neurogenesis during brain development, some GFAP$^+$ precursors might have undergone irreversible recombination, leading to inadvertent expression of DTR in mature neurons of GFAP:iDTR mice. Bajenaru et al. (2002) reported that the GFAPCre strain used here does not induce any obvious neuronal expression of a *loxP*-flanked transgene. However, to definitively rule out potential, neuronal DTR expression, we used a second model, by which tamoxifen-inducible Cre-ERT2 allows temporarily precise postnatal induction of DTA expression in adult astrocytes (GFAPCreERT2:DTA; Hirrlinger et al., 2006; Ivanova et al., 2005; Figure 1A).

As the most-pronounced pathology in tamoxifen-treated GFAPCreERT2:DTA mice was found in the cervical spinal cord, our subsequent analysis focused on this region. We confirmed the specificity of this genetic targeting approach by flow cytometry and immunohistochemical analysis of GFAPCreERT2 mice crossed to a Rosa26-tdTomato reporter mouse line (Figures 1B and S2). In the spinal cord, the Cre-recombinase was primarily active in the subpopulation of GFAP$^+$ astrocytes (79% ± 3.6% of which were tdTomato$^+$; n = 6 mice), whereas only a smaller fraction of astrocytes (23% ± 2.5% of which were tdTomato$^+$; n = 6 mice) labeled with the more-abundant marker S100$^+$ were targeted (Figure 1B). Our results further showed that, at

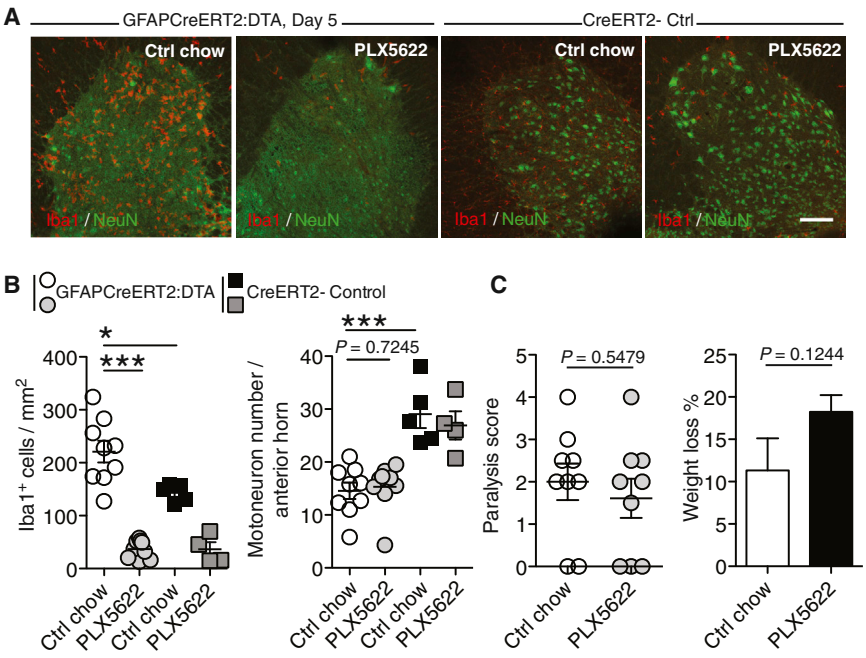

Figure 2. Motoneuron Loss in Spinal Cords of GFAPCreERT2:DTA Mice Is Independent of Microglial Bystander Activation

GFAPCreERT2:DTA (n = 9/group) and CreERT2-control mice (n = 4 to 5/group) were pre-/treated with the oral CSF1R inhibitor PLX5622 (1.2 g/kg chow) or vehicle for 1 week to eliminate microglia and kept on this diet throughout the experiment.

(A) Representative Iba1 and NeuN immunofluorescent stainings from the anterior horn region at day 5 of tamoxifen i.p. application showing loss of moto-/neurons despite robust decreases in microglial numbers.

(B) Quantifications of Iba1$^+$ and motoneuron cell bodies.

(C) There was no statistical difference in paralysis scores at day 5 between PLX5622- and vehicle-treated GFAPCreERT2:DTA mice.

Mice were pooled from two independent experiments, and asterisks indicate significance by unpaired Student's t test; *p < 0.05; ***p < 0.001. Error bars represent mean ± SEM. The scale bars represent 100 μm (A). See also Figure S3.

day 6 after the start of tamoxifen treatment, the expression of DTA toxin leads to significantly reduced tdTomato$^+$ cell numbers compared to controls (by 73%; Figures 1B and 1C). This suggested that a substantial fraction of GFAP$^+$ astrocytes, in which the Cre recombinase was active, were dying or in an inanimate state with blocked (reporter) protein synthesis. i.p. injections of tamoxifen in GFAPCreERT2:DTA mice resulted in a rapid and severe paresis that started asymmetrically in both upper limbs, later progressed to all four extremities (onset at days 5–8), and was accompanied by weight loss (Figure 1D). In the spinal cord, we found that the numbers of neurons (by 63%) and oligodendrocytes (by 55%) were reduced at day 6, paralleling the appearance of the clinical phenotype. In contrast, a comparable number of S100$^+$ astrocytes (of which only few express the Cre recombinase and the loss of which is therefore likely obscured by a gliotic response) was present at all time points, suggesting that an overall astroglial support structure persisted (Figures 1E and 1F).

The GFAPCre:iDTR mice were used to confirm the specificity of the genetic targeting through the GFAP promoter and additionally permitted region-specific application of DT (for details, see Figure S1). Of note, the model validated our finding that paralysis of GFAP$^+$ astrocytes leads to rapid and fulminant neuronal demise. However, for the remainder of this report, we focused on the analysis of GFAPCreERT2:DTA mice.

Neuronal Loss and Clinical Deficits Occur Independent of Microglial Activation and Proliferation

Given the observed morphological activation and proliferation of microglia (Figures 1E and 1F), we reasoned whether microglial-derived factors contributed to neuronal demise and the functional deficits in GFAPCreERT2:DTA mice. To directly assess the role of microglia in astrocyte-driven motoneuron injury in our model, we used the colony-stimulating factor 1 receptor (CSF1R) antagonist PLX5622, which has been shown to efficiently eliminate microglia from the adult brain (Elmore et al., 2014). We conducted a 7-day treatment in control wild-type mice and confirmed microglial depletion in isolated spinal cords by flow cytometry (not shown). We then administered PLX5622-containing or control chow to GFAPCreERT2:DTA mice 8 days before tamoxifen induction (i.p. injected at days 1–5) and throughout the experiment (Figures 2A–2C). CSFR1 blockade decreased microglial content at day 5, as assessed by the number of Iba1$^+$ cells in cervical sections (by 83% in GFAP-CreERT2:DTA and by 74% in CreERT2-control mice). However, at the same time point, the loss in motoneuron numbers and the severity of clinical paralysis was not significantly different from mice fed with control chow (Figures 2B and 2C). These findings indicate that, in our model, microglia are rather bystanders and do not actively contribute to the initiation of neuronal injury and clinical deficits.

Neuronal Loss after Paralysis of GFAP$^+$ Astrocytes Does Not Correlate with CNS Vascular Leakage or Reduction in Glutamate-Detoxifying Enzyme Levels

A number of astrocyte properties are likely important for maintaining neuronal health in the adult nervous system. To discern which disturbed function of GFAP$^+$ astrocytes is responsible for the rapid neuronal cell loss observed in our model, we next investigated the vascular integrity in the CNS of GFAP-CreERT2:DTA mice (Figures S3A–S3C). Astrocytes are integral components of the neurovascular unit, and leakage of serum proteins has been implicated in neuronal damage (Paul et al., 2007). Even in areas exhibiting substantial loss of neurons, vascular basal lamina collagen-IV and endothelial glucose transporter 1 (GLUT-1) (Figure S3A) expression were unaltered. We

did not observe perivascular deposits of plasma-derived IgG, even at time points when blood vessels were stripped of GFAP$^+$ processes (Figure S3A). Consistent with a mostly intact neurovascular unit, there were no spontaneous microbleeds (Figure S3A) or leukocyte extravasation (Figure S3B). We found reduced protein contents of the tight junction component occludin, which has been shown to be expressed by cultured astrocytes (Wachtel et al., 2001), but unaltered claudin 5 levels and no accumulation of fibrinogen in spinal cord tissue (Figure S3C). Whereas these data do not dismiss the importance of astrocytes for the full functioning of the neurovascular unit, they do suggest that neuronal injury in our model was not primarily driven by microvascular damage and leakage of toxic blood products.

The uptake of the potentially toxic neurotransmitter glutamate has been suggested as another important homeostatic function of astrocytes in the CNS (Mennerick and Zorumski, 1994), and failure to eliminate glutamate has been proposed to contribute to several neurodegenerative disorders, such as amyotrophic lateral sclerosis (Rothstein et al., 1995) or spinocerebellar ataxia 7 (Custer et al., 2006). We performed immunohistochemical stainings for glutamine synthetase (GS), an astroglial enzyme that rapidly converts excess glutamate into glutamine, in spinal cord regions, where extensive neuronal loss could be found. Co-labeling revealed that a considerable proportion of GS-immunoreactive glial cells did not express GFAP in the spinal cord area of interest (Figure S3D). Indeed, densities of GS$^+$ cells were unaltered compared to controls (Figures S3D and S3E) around 1 week after the induction of GFAP$^+$ astrocyte paralysis. These results suggested that, despite GFAP$^+$ astrocyte paralysis, the remaining glial pool retains its capacity to detoxify glutamate at least during the time period in which neuronal damage was initiated in our model.

GFAP$^+$ Astroglial Paralysis and Neuronal Damage Are Associated with Decreased Capabilities to Neutralize ROS/RNS

Reactive oxygen and nitrogen species (ROS/RNS) are another group of potentially harmful molecules that need to be efficiently scavenged to prevent the occurrence of oxidative stress. To assess the redox-scavenging capacity of astrocytes, we therefore quantified the basal mRNA expression of ROS-detoxifying enzymes in the glial cell population in our GFAPCreERT2:DTA model, using the predominantly astroglial transporter GLAST as a marker for sorting and excluding CD45^{low}CD11b$^+$ microglia cells (Figure S4). Superoxide dismutase SOD1, SOD2, and catalase mRNA levels were approximately three to four times higher in GLAST$^+$ glia compared to microglia sorted from the CNS of GFAPCreERT2:DTA and control mice (Figure 3A). Tamoxifen-treatment reduced mRNA expression in GLAST$^+$ glia by 34% (SOD1), 47% (SOD2), or 71% (catalase). This reduction in the glial cell pool was confirmed by intracellular protein staining for SOD1 and SOD2 (Figure 3B). In contrast, microglial expression of redox-scavenging enzymes was not affected (Figures 3A and 3B). Flow cytometric analysis of GFAPCreERT2:DTA and GFAPCreERT2 control mice crossed with the Rosa26-tdTomato reporter mouse line confirmed that tdTomato$^+$SOD1$^+$ and SOD2$^+$ astrocytes vanished after tamoxifen treatment of GFAP-CreERT2:DTA mice (Figure 3C). Diminished ROS-scavenging capabilities in GFAPCreERT2:DTA mice were accompanied by increased superoxide levels and enhanced oxidative DNA damage (Figures 3D and 3E). A disturbed redox balance in our model would also be consistent with the ultrastructural signs of abnormal autophagic activity that we observed in degenerating neurons (Figures 3F–3H; Scherz-Shouval et al., 2007). To evaluate the effect of ROS/RNS scavengers in vivo, mice were treated i.p. with a ROS/RNS scavenger cocktail containing FeTPPS, EUK134, and PBN starting from the day of tamoxifen application (Nikić et al., 2011). Compared to the vehicle-treated cohort, ROS/RNS scavenger-treated mice showed a significantly increased number of surviving neurons including a preservation of motoneurons, whereas the number of astrocytes, oligodendrocytes, and microglial cells were not affected (Figures 4A and 4B). In addition, we measured serum concentrations of neuron-specific enolase (NSE), which is systemically released upon neuronal injury. NSE serum levels in GFAPCreERT2:DTA mice were significantly increased compared to CreERT2$^-$ controls (Figure 4C) with mean NSE levels lying between values reported for models of ischemic stroke and inflammatory CNS insults (Gelderblom et al., 2013). Again treatment with ROS/RNS scavengers reduced serum NSE levels by approximately 75% (Figure 4C). ROS/RNS scavenging not only improved neuronal survival but also prevented clinical deficits (at days 5 or 6; Figure 4D). Taken together, these data indicate that neuronal damage and the resulting clinical paralysis in our model is at least partly caused by the disturbed redox homeostasis that results from paralysis of GFAP$^+$ astrocytes.

DISCUSSION

Whereas it is becoming increasingly clear that astrocytes play an important role in a number of neurological disorders, their contribution to tissue homeostasis in the healthy nervous system is still not fully understood. Here, we addressed this question by genetically paralyzing and depleting GFAP$^+$ astrocytes in adult mice in vivo. Using this method has proven to be valuable to understand the role of microglia (Parkhurst et al., 2013), mature oligodendrocytes (Locatelli et al., 2012), or neuronal subpopulations like agouti-related protein (ARP)$^+$ neurons (Gropp et al., 2005) in the adult CNS. In all those depletion models, the mice were viable and displayed, if any, only subtle clinical phenotypes under steady-state conditions. We set out to target and reduce GFAP$^+$ astrocytes, which, depending on the CNS region, comprise only a fraction of all astrocytes (Cahoy et al., 2008). Yet, our results provide direct evidence that, different from other glial cell types in the CNS, GFAP$^+$ astrocytes are far more critical for neuronal integrity in adult mammals.

We observed a rapid onset of severe motor deficits that was accompanied by early neuronal injury and substantial cell loss. This phenotype contrasts with what is observed after induced depletion of pMN-derived AldoC$^+$ astrocytes (*Olig2-cre:Aldh1L1-DTA*; Tsai et al., 2012), where sizes and numbers of motoneurons in spinal cord ventral horns remained unaffected. This discrepancy is likely to arise from the fact that distinct subsets of astrocytes are targeted and that there are potential compensatory events in place when astroglial cells are affected during embryonic development. Experiments aiming

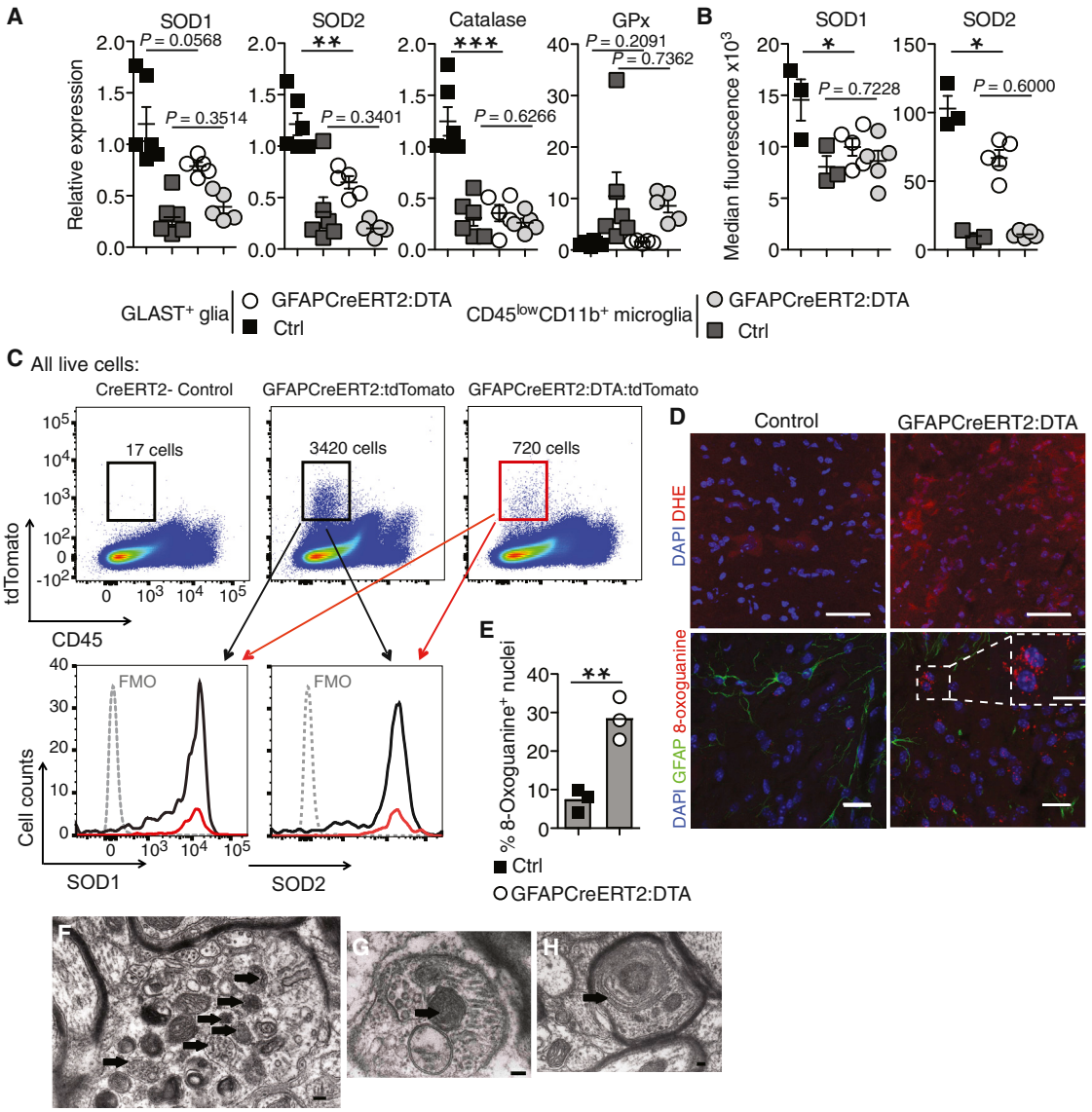

Figure 3. Reduced Glial ROS-Scavenging Capabilities in GFAPCreERT2:DTA Mice

(A and B) The relative expression of various detoxifying enzymes of the ROS defense system were reduced in the sorted GLAST$^+$ glial cell pool from the CNS of GFAPCreERT2:DTA mice at days 5 to 6 compared with CreERT2- controls as determined by (A) real-time PCR analysis, (B) intracellular staining, and flow cytometry (mean ± SEM; n = 3–6 mice/group). GPx, glutathione peroxidase.

(C) For confirmation, the absolute number of SOD$^+$ tdTomato$^+$ astrocytes of the CNS glial population was determined by flow cytometry using GFAPCreERT2:DTA:tdTomato and control mice (representative sample; n = 2 per group). FMO, fluorescence minus one staining.

(D) This was accompanied by increased labeling of cervical spinal cord sections with the fluorescent ROS probe DHE or the oxidative-stress marker 8-oxoguanine.

(E) Quantifications of 8-oxoguanine$^+$ nuclei (n = 3 mice/group; individual mice represented by squares and circles; average of six to seven sections/mouse).

(F) Electron microscopy of a large dystrophic neurite containing autolysosomes and electron-dense and numerous enlarged multivesicular bodies (arrows).

(G and H) Mitochondria surrounded by membranes (arrows) indicating early autophagy.

The scale bars represent 50 μm (DHE; D), 20 μm (8-oxoguanine; D), 10 μm (zoom; D), and 200 nm (F–H). p values for unpaired comparisons were analyzed by two-tailed Student's t test. *p < 0.05; **p < 0.01; ***p < 0.001. See also Figure S4.

to remove certain intermediate filaments already indicated that the full integrity of the astrocyte cytoskeleton in the absence of further injury is largely irrelevant for neuronal survival (Colucci-Guyon et al., 1994; Pekny et al., 1995). Our findings support this notion, as neuronal damage in the experimental procedures here occurred despite persistence of an astroglial support structure, in part provided by remaining GFAP$^-$ astrocyte populations and the mostly intact CNS microvasculature.

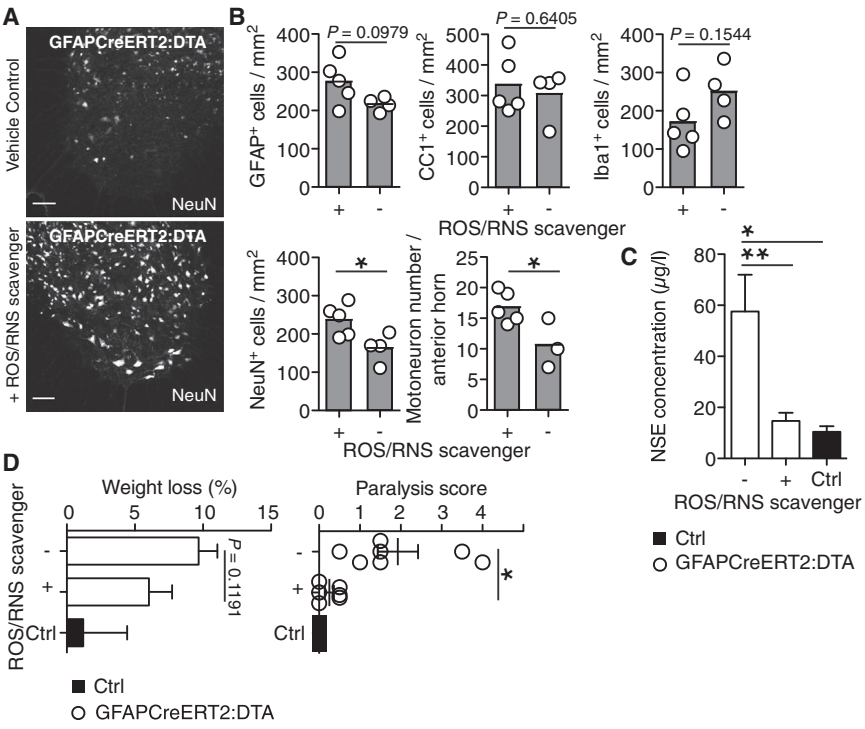

Figure 4. Neutralization of ROS and RNS Rescues Neurons in GFAPCreERT2:DTA Mice

(A and B) Glial and neuronal cell numbers after i.p. (+) ROS/RNS scavenger or (−) vehicle treatment (n = 4 to 5 mice/group). NeuN-positive neurons and motoneurons per anterior horn were significantly increased by ROS/RNS scavenging (n ≥ 3 mice/group).

(C) Extent of neuronal injury quantified by serum levels of NSE (mean ± SEM; serum from n = 8–14 mice/group).

(D) Weight and paralysis score at days 5 to 6 (clinical onset; mean ± SEM; n = 6 to 7 mice/group).

The scale bars represent 100 μm (A). p values for unpaired comparisons were analyzed by two-tailed Student's t test. *p < 0.05; **p < 0.01.

Microglia activation is present in the vicinity of the degenerating motoneurons, for example in amyotrophic lateral sclerosis (Troost et al., 1990). Our results show that, after astrocyte paralysis, microglia respond early to disturbed CNS homeostasis and become activated even before neuronal injury is obvious. Although treatment with an oral CSFR1 inhibitor virtually abolished microglial activation and proliferation, spinal cord motoneurons died and clinical paralysis developed. Even though our findings clearly do not exclude a role of microglia in the propagation of other neurodegenerative conditions, they indicate that, in our relatively rapid model of astrocyte paralysis-induced motoneuron death, microglia are not critical players.

What are the mechanisms of astrocyte paralysis-mediated neuronal damage? Astrocytes synthesize a plethora of factors that have been shown, still mostly in vitro, to be important for neuronal and synaptic integrity (Allen et al., 2012; Christopherson et al., 2005). Although acute inhibition of astrocyte protein synthesis might result in lack of trophic support for neurons, it is equally likely that it leads to inactivation of glial-detoxifying pathways. Mutations in SOD1 cause a rare form of familial amyotrophic lateral sclerosis, and studies using transgenic rodents expressing mutant human SOD1 have indeed demonstrated that motoneurons are particularly vulnerable to toxic activity mediated by astrocytes (Gurney et al., 1994; Nagai et al., 2007). Previous co-culture experiments suggested that neurons depend on the antioxidant potential of astrocytes for their own defense against oxidative stress in vitro (Desagher et al., 1996). Of the potential mechanisms studied here, we found a critical involvement of astrocytes in redox homeostasis and that the lesioning of adult astrocytes in vivo leads to oxidative stress and neuronal decline.

In summary, our study identifies the redox-scavenging capacity of GFAP+ astrocytes as a key contributor to CNS homeostasis and suggests that the pure scaffold function of astrocytes is much less critical to neuronal health than the metabolic integrity of the glia-neuron interface. From a translational viewpoint, our findings have implications not only for neurodegenerative diseases such as amyotrophic lateral sclerosis but also for neuroprotective interventions that might be more likely to succeed if they target not only neurons but also their glial environment.

EXPERIMENTAL PROCEDURES

In Vivo Treatments

All procedures involving animals were approved by the veterinary office of the Canton of Zurich, Switzerland. GFAPCreERT2:DTA mice were i.p. injected with a tamoxifen dosage of 2 mg/day for 5 days on a daily basis (days 1–5). To eliminate microglia, mice were treated with the CSF1R antagonist, PLX5622 (Plexxikon), formulated in AIN-76A rodent chow (Research Diets) at a dose of 1.2 g/kg. To scavenge ROS and/or RNS, we i.p. injected a cocktail containing FeTTPS (5,10,15,20-tetrakis(4-sulfonatophenyl)porphyrinato iron (III), chloride; Calbiochem), a peroxynitrate scavenger, PBN (*N*-*tert*-butyl-α-phenylnitrone; Sigma-Aldrich), a spin trap that reacts with superoxide and hydroxyl radicals, and EUK134 (Cayman Chemicals), a catalase and superoxide dismutase analog, as described in detail in Nikić et al. (2011).

Clinical Scoring

Paralysis scores of GFAPCreERT2:DTA mice were assessed on a scale from 0 to 5, with 0 indicating no detectable signs, 1 paresis of one front limb, 2 paresis of two front limbs, 3 complete bilateral front limb paralysis, 3.5 complete bilateral front limb paralysis and partial hind limb paralysis, 4 tetraparalysis, and 5 dead. For additional details, please see the Supplemental Experimental Procedures.

Immunohistochemistry, Image Acquisition, and Quantifications

Immunohistochemistry was performed following standard methods. For further information including antibodies dilutions, clones, and/or companies, we refer to the Supplemental Experimental Procedures. The superoxide indicator dihydroethidium (DHE; Sigma-Aldrich) was injected at 1 mg/ml (200 μl/mouse) i.p. or i.v. After 30–90 min, mice were intracardially perfused

with PBS and spinal cords frozen in OCT compound prior to cryostat sectioning and mild fixation with 2% PFA.

Images were processed and merged by Imaris imaging software (version 7.5.1; Bitplane). Cells were counted manually, or quantifications were done automatically using Imaris or Fiji/ImageJ 1.46j (NIH) software.

Transmission Electron Microscopy

Transmission electron microscopy was performed as previously described (Locatelli et al., 2012).

CNS Flow Cytometry

We homogenized adult brain and spinal cord tissues and removed the myelin using a 30% Percoll gradient. For further information on cytometric analysis including antibodies clones and/or companies, we refer to the Supplemental Experimental Procedures. Cell sorting was carried out using a FACSAria III (BD). The gating strategy of GLAST^{+} astrocyte FACS-isolation is depicted in Figure S4. Data analysis was done using FlowJo X 10.0.7 (Treestar).

NSE ELISA

NSE concentrations were determined in serum samples using the CanAg NSE EIA (Fujirebio) as described (Gelderblom et al., 2013).

Real-Time qPCR

Total RNA was purified from sorted cells with the RNeasy Micro kit (QIAGEN) according to the manufacturer's instructions. The RNA from individual, single mice was isolated, cDNA synthesized, and real-time PCR done in triplicates using a CFX384 Cycler (Bio-Rad). The results were normalized to those of an internal control (DNA polymerase II), and then transcripts in each sample were normalized to a calibrator sample.

Statistical Analysis

Statistical significance was determined with GraphPad Prism (GraphPad Software). Unpaired two-tailed Student's t tests or one-way ANOVA tests with Dunnett's multiple comparison test were performed to analyze significance between experimental and control groups. Two-way repeated-measures ANOVA tests were used to detect interactions between time and genotype.

For additional details, please see the Supplemental Experimental Procedures.

SUPPLEMENTAL INFORMATION

Supplemental Information includes Supplemental Experimental Procedures and four figures and can be found with this article online at http://dx.doi.org/10.1016/j.celrep.2015.07.051.

AUTHOR CONTRIBUTIONS

B.S. and E.R. designed, performed, and interpreted experiments. B.S., E.R., M.K., and B.B. wrote the manuscript. P.L. performed the TEM analysis. B.I.-H., B.S.-B., T.H., V.C., and H.J. helped perform and analyze experiments. H.U.Z., A.A., and F.H. helped revise the manuscript. B.B. directed and financed the study.

ACKNOWLEDGMENTS

We are grateful to Sabrina Nemetz Hasler and Paulina Kulig for excellent technical help. We thank the Center for Microscopy and Image Analysis at the University of Zurich. We thank Plexxikon (Parmveer Singh and Dr. Brian West) for freely and openly providing PLX5622-containing and control diets. This study was supported by grants from the Swiss National Science Foundation (316030_150768 [to B.B.], 310030_146130 [to B.B.], and CRSII3_136203 [to B.B.]), Special Program University Medicine (SPUM), European Union FP7 project TargetBraIn, NeuroKine and ATECT (to B.B.), the Stiftung für Forschung an der Medizinischen Fakultät of the University of Zurich (to B.S.), and Bayer Health Care (ISS 14500 [to B.S.]). P.L. is partially supported by the Healthy Ageing Research Center (HARC).

Received: November 19, 2014
Revised: July 1, 2015
Accepted: July 24, 2015
Published: August 20, 2015

REFERENCES

Allen, N.J., and Barres, B.A. (2009). Neuroscience: Glia - more than just brain glue. Nature *457*, 675–677.

Allen, N.J., Bennett, M.L., Foo, L.C., Wang, G.X., Chakraborty, C., Smith, S.J., and Barres, B.A. (2012). Astrocyte glypicans 4 and 6 promote formation of excitatory synapses via GluA1 AMPA receptors. Nature *486*, 410–414.

Bajenaru, M.L., Zhu, Y., Hedrick, N.M., Donahoe, J., Parada, L.F., and Gutmann, D.H. (2002). Astrocyte-specific inactivation of the neurofibromatosis 1 gene (NF1) is insufficient for astrocytoma formation. Mol. Cell. Biol. *22*, 5100–5113.

Banker, G.A. (1980). Trophic interactions between astroglial cells and hippocampal neurons in culture. Science *209*, 809–810.

Buch, T., Heppner, F.L., Tertilt, C., Heinen, T.J., Kremer, M., Wunderlich, F.T., Jung, S., and Waisman, A. (2005). A Cre-inducible diphtheria toxin receptor mediates cell lineage ablation after toxin administration. Nat. Methods *2*, 419–426.

Bush, T.G., Puvanachandra, N., Horner, C.H., Polito, A., Ostenfeld, T., Svendsen, C.N., Mucke, L., Johnson, M.H., and Sofroniew, M.V. (1999). Leukocyte infiltration, neuronal degeneration, and neurite outgrowth after ablation of scar-forming, reactive astrocytes in adult transgenic mice. Neuron *23*, 297–308.

Cahoy, J.D., Emery, B., Kaushal, A., Foo, L.C., Zamanian, J.L., Christopherson, K.S., Xing, Y., Lubischer, J.L., Krieg, P.A., Krupenko, S.A., et al. (2008). A transcriptome database for astrocytes, neurons, and oligodendrocytes: a new resource for understanding brain development and function. J. Neurosci. *28*, 264–278.

Christopherson, K.S., Ullian, E.M., Stokes, C.C., Mullowney, C.E., Hell, J.W., Agah, A., Lawler, J., Mosher, D.F., Bornstein, P., and Barres, B.A. (2005). Thrombospondins are astrocyte-secreted proteins that promote CNS synaptogenesis. Cell *120*, 421–433.

Colucci-Guyon, E., Portier, M.M., Dunia, I., Paulin, D., Pournin, S., and Babinet, C. (1994). Mice lacking vimentin develop and reproduce without an obvious phenotype. Cell *79*, 679–694.

Custer, S.K., Garden, G.A., Gill, N., Rueb, U., Libby, R.T., Schultz, C., Guyenet, S.J., Deller, T., Westrum, L.E., Sopher, B.L., and La Spada, A.R. (2006). Bergmann glia expression of polyglutamine-expanded ataxin-7 produces neurodegeneration by impairing glutamate transport. Nat. Neurosci. *9*, 1302–1311.

Desagher, S., Glowinski, J., and Premont, J. (1996). Astrocytes protect neurons from hydrogen peroxide toxicity. J. Neurosci. *16*, 2553–2562.

Elmore, M.R., Najafi, A.R., Koike, M.A., Dagher, N.N., Spangenberg, E.E., Rice, R.A., Kitazawa, M., Matusow, B., Nguyen, H., West, B.L., and Green, K.N. (2014). Colony-stimulating factor 1 receptor signaling is necessary for microglia viability, unmasking a microglia progenitor cell in the adult brain. Neuron *82*, 380–397.

Gelderblom, M., Daehn, T., Schattling, B., Ludewig, P., Bernreuther, C., Arunachalam, P., Matschke, J., Glatzel, M., Gerloff, C., Friese, M.A., and Magnus, T. (2013). Plasma levels of neuron specific enolase quantify the extent of neuronal injury in murine models of ischemic stroke and multiple sclerosis. Neurobiol. Dis. *59*, 177–182.

Gropp, E., Shanabrough, M., Borok, E., Xu, A.W., Janoschek, R., Buch, T., Plum, L., Balthasar, N., Hampel, B., Waisman, A., et al. (2005). Agouti-related peptide-expressing neurons are mandatory for feeding. Nat. Neurosci. *8*, 1289–1291.

Gurney, M.E., Pu, H., Chiu, A.Y., Dal Canto, M.C., Polchow, C.Y., Alexander, D.D., Caliendo, J., Hentati, A., Kwon, Y.W., Deng, H.X., et al. (1994). Motor

neuron degeneration in mice that express a human Cu,Zn superoxide dismutase mutation. Science *264*, 1772–1775.

Haidet-Phillips, A.M., Hester, M.E., Miranda, C.J., Meyer, K., Braun, L., Frakes, A., Song, S., Likhite, S., Murtha, M.J., Foust, K.D., et al. (2011). Astrocytes from familial and sporadic ALS patients are toxic to motor neurons. Nat. Biotechnol. *29*, 824–828.

Hirrlinger, P.G., Scheller, A., Braun, C., Hirrlinger, J., and Kirchhoff, F. (2006). Temporal control of gene recombination in astrocytes by transgenic expression of the tamoxifen-inducible DNA recombinase variant CreERT2. Glia *54*, 11–20.

Honjo, T., Nishizuka, Y., Kato, I., and Hayaishi, O. (1971). Adenosine diphosphate ribosylation of aminoacyl transferase II and inhibition of protein synthesis by diphtheria toxin. J. Biol. Chem. *246*, 4251–4260.

Ivanova, A., Signore, M., Caro, N., Greene, N.D., Copp, A.J., and Martinez-Barbera, J.P. (2005). In vivo genetic ablation by Cre-mediated expression of diphtheria toxin fragment A. Genesis *43*, 129–135.

Locatelli, G., Wörtge, S., Buch, T., Ingold, B., Frommer, F., Sobottka, B., Krüger, M., Karram, K., Bühlmann, C., Bechmann, I., et al. (2012). Primary oligodendrocyte death does not elicit anti-CNS immunity. Nat. Neurosci. *15*, 543–550.

Mennerick, S., and Zorumski, C.F. (1994). Glial contributions to excitatory neurotransmission in cultured hippocampal cells. Nature *368*, 59–62.

Nagai, M., Re, D.B., Nagata, T., Chalazonitis, A., Jessell, T.M., Wichterle, H., and Przedborski, S. (2007). Astrocytes expressing ALS-linked mutated SOD1 release factors selectively toxic to motor neurons. Nat. Neurosci. *10*, 615–622.

Nikić, I., Merkler, D., Sorbara, C., Brinkoetter, M., Kreutzfeldt, M., Bareyre, F.M., Brück, W., Bishop, D., Misgeld, T., and Kerschensteiner, M. (2011). A reversible form of axon damage in experimental autoimmune encephalomyelitis and multiple sclerosis. Nat. Med. *17*, 495–499.

Parkhurst, C.N., Yang, G., Ninan, I., Savas, J.N., Yates, J.R., 3rd, Lafaille, J.J., Hempstead, B.L., Littman, D.R., and Gan, W.B. (2013). Microglia promote learning-dependent synapse formation through brain-derived neurotrophic factor. Cell *155*, 1596–1609.

Paul, J., Strickland, S., and Melchor, J.P. (2007). Fibrin deposition accelerates neurovascular damage and neuroinflammation in mouse models of Alzheimer's disease. J. Exp. Med. *204*, 1999–2008.

Pekny, M., Levéen, P., Pekna, M., Eliasson, C., Berthold, C.H., Westermark, B., and Betsholtz, C. (1995). Mice lacking glial fibrillary acidic protein display astrocytes devoid of intermediate filaments but develop and reproduce normally. EMBO J. *14*, 1590–1598.

Rothstein, J.D., Van Kammen, M., Levey, A.I., Martin, L.J., and Kuncl, R.W. (1995). Selective loss of glial glutamate transporter GLT-1 in amyotrophic lateral sclerosis. Ann. Neurol. *38*, 73–84.

Scherz-Shouval, R., Shvets, E., Fass, E., Shorer, H., Gil, L., and Elazar, Z. (2007). Reactive oxygen species are essential for autophagy and specifically regulate the activity of Atg4. EMBO J. *26*, 1749–1760.

Sofroniew, M.V., and Vinters, H.V. (2010). Astrocytes: biology and pathology. Acta Neuropathol. *119*, 7–35.

Sorensen, A., Moffat, K., Thomson, C., and Barnett, S.C. (2008). Astrocytes, but not olfactory ensheathing cells or Schwann cells, promote myelination of CNS axons in vitro. Glia *56*, 750–763.

Troost, D., Van den Oord, J.J., and Vianney de Jong, J.M. (1990). Immunohistochemical characterization of the inflammatory infiltrate in amyotrophic lateral sclerosis. Neuropathol. Appl. Neurobiol. *16*, 401–410.

Tsai, H.H., Li, H., Fuentealba, L.C., Molofsky, A.V., Taveira-Marques, R., Zhuang, H., Tenney, A., Murnen, A.T., Fancy, S.P., Merkle, F., et al. (2012). Regional astrocyte allocation regulates CNS synaptogenesis and repair. Science *337*, 358–362.

Wachtel, M., Bolliger, M.F., Ishihara, H., Frei, K., Bluethmann, H., and Gloor, S.M. (2001). Down-regulation of occludin expression in astrocytes by tumour necrosis factor (TNF) is mediated via TNF type-1 receptor and nuclear factor-kappaB activation. J. Neurochem. *78*, 155–162.